Approximate method for calculating the radiation from a moving charge in the presence of a complex object

Ekaterina S. Belonogaya[*]
Physical Faculty of St. Petersburg State University, St. Petersburg 198504, Russia and
Saint Petersburg State Electrotechnical University "LETI", St. Petersburg 197376, Russia

Andrey V. Tyukhtin[†] and Sergey N. Galyamin[‡]
Physical Faculty of St. Petersburg State University, St. Petersburg 198504, Russia
(Received 28 January 2013; published 12 April 2013)

An approximate method for calculating the radiation from a moving charge in the presence of a dielectric object is developed. The method is composed of two steps. The first step is calculation of the field in the medium without considering the external boundaries of the object, and the second step is an approximate (ray-optical) calculation of the wave propagation outside the object. As a test problem, we consider the case of a charge crossing a dielectric plate. Computations of the field are performed using exact and approximate methods. It is shown that the results agree well. Additionally, we apply the method under consideration to the case of a cone-shaped object with a vacuum channel. The radiation energy spectral density as a function of the location of the observation point and the problem's parameters is given. In particular, the convergent radiation effect is described.

DOI: 10.1103/PhysRevE.87.043201 PACS number(s): 41.20.−q, 42.15.−i, 41.60.Bq

I. INTRODUCTION

Problems of radiation from charged particles in the presence of dielectric objects are of interest for a series of important applications in accelerator and beam physics and other areas. For example, such problems are typical of Cherenkov detectors [1]. Additionally, a recently reported method for bunch diagnostics is connected to these problems [2].

It should be noted that, as a rule, the radiation field is measured outside the dielectric object. The form of the object in such problems usually does not allow an exact analytical solution to be obtained. At the same time, computer simulation of electromagnetic fields is very cumbersome. Thus, the development of approximate methods for calculating the field of a moving bunch in the presence of different dielectric objects is of great interest. One such technique is offered and developed in this paper.

The method under consideration can be used for at least the following situations: (1) a charge moving into some dielectric or magnetic object, (2) a charge moving in a vacuum channel in such an object, and (3) a charge moving along the border of an object. The radius of the channel (in the second situation) and the distance from the border (in the third situation) can be, in principle, arbitrary. Note that the cases when these parameters are relatively small (no more than the wavelength under consideration λ) are of most interest because radiation is exponentially small if these parameters are much more than λ.

In any case, we assume that Cherenkov radiation (CR) is generated in the object but is not excited outside it. Such a situation usually occurs in problems concerning Cherenkov detectors [1] and in schemes for diagnostics of charged particle bunches [2].

The method offered here concerns problems that are characterized by some large geometric parameter: the size of the object is assumed to be much larger than the wavelengths under consideration. To be more exact, it is assumed that the CR excited by the bunch travels into the object over a distance that is much longer than the typical wavelengths. It should be emphasized that the other geometric parameters (such as the channel radius or the distance from the object's border to the charge trajectory) can be arbitrary.

Under such conditions, the following approach can be applied. At first, the field of the charge in an infinite medium without "external" borders is calculated. It is important that the finite distance from the charge trajectory to the nearest border of the object is taken into account in this step.

The second step is the approximate calculation of the radiation exiting the object (sometimes named "Cherenkov-transition radiation" (CTR) [3,4]). This calculation is related to Fock's method for analyzing reflection of waves from an arbitrary surface [5], but we address transmission instead of reflection. Analogous calculations are applied to elaborate different optical systems [6]. The incident field is multiplied by the Fresnel transmission coefficient, and then the decrease (or increase) in the radiation field because of change in the ray tube cross section in the external medium is taken into account. Thus, the first of the CTR refracted rays is obtained. This ray will most likely be satisfactory for the majority of applied problems. If necessary, multiple reflections and refractions from the object's borders can be taken into account.

II. EXACT SOLUTION FOR A DIELECTRIC PLATE

To test the method under consideration, we use the problem of the field of a point charge flying through a dielectric layer placed at $0 < z < d$ (Fig. 1). The medium of the layer has permittivity ε_2 and permeability μ_2, and the half-spaces outside the layer are characterized by permittivity ε_1 and

[*]ekaterinabelonogaya@yandex.ru
[†]tyukhtin@bk.ru
[‡]galiaminsn@yandex.ru

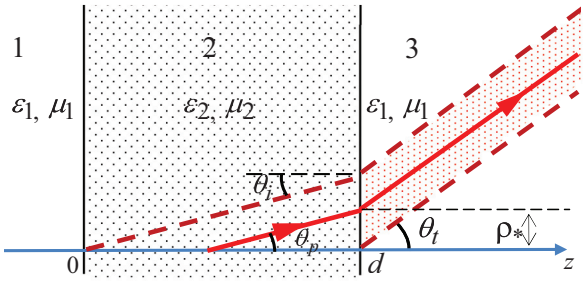

FIG. 1. (Color online) Cross section of the plate. The region enclosed by dashed lines is the zone of the first ray.

permeability μ_1. A point charge q moves perpendicularly to the layer with a constant velocity V. The charge's location at time t is determined by the equations $x = y = 0$ and $z = Vt$, so the charge density is written in the form $\rho = q\delta(x,y,z-Vt)$. The tangential projections of the electric and magnetic fields should be continuous at the layer boundaries.

Such a problem has an exact solution [7], which has been independently proved by us. To calculate the field, the scalar (Φ) and vector ($\vec{A}_z = A_z\vec{e}_z$) potentials were used, and the Fourier method was applied. The solution can be written as the sum of a "forced" field (the field of the charge in an unbounded medium) and a "free" field (which is connected with the influence of the boundaries). The forced-field potentials have the form

$$\begin{Bmatrix} A_z^{(1),(3)} \\ \Phi^{(1),(3)} \end{Bmatrix} = \frac{q}{2\pi^2 V}\int_0^{+\infty}\int_0^{2\pi}\int_{-\infty}^{+\infty}\begin{Bmatrix} \mu_1\beta \\ 1/\varepsilon_1 \end{Bmatrix} g_1^{-1}k_\rho \times \exp\left(i\frac{\omega}{V}z + i\vec{k}_\rho\vec{\rho} - i\omega t\right)dk_\rho d\phi_k d\omega, \quad (1)$$

$$\begin{Bmatrix} A_z^{(2)} \\ \Phi^{(2)} \end{Bmatrix} = \frac{q}{2\pi^2 V}\int_0^{+\infty}\int_0^{2\pi}\int_{-\infty}^{+\infty}\begin{Bmatrix} \mu_2\beta \\ 1/\varepsilon_2 \end{Bmatrix} g_2^{-1}k_\rho \times \exp\left(i\frac{\omega}{V}z + i\vec{k}_\rho\vec{\rho} - i\omega t\right)dk_\rho d\phi_k d\omega, \quad (2)$$

where the indexes (1), (2), and (3) refer to regions 1, 2, and 3, respectively (Fig. 1), and ρ, ϕ, z are cylindrical coordinates. The free-field potentials have the following form:

$$\begin{Bmatrix} A_z^{(s1)} \\ \Phi^{(s1)} \end{Bmatrix} = \frac{q}{2\pi^2 V}\int_0^{+\infty}\int_0^{2\pi}\int_{-\infty}^{+\infty} V_1\begin{Bmatrix} \mu_1/k_z^{(1)} \\ c/\omega\varepsilon_1 \end{Bmatrix} g_1^{-1}k_\rho \times \exp\left(-ik_z^{(1)}|z| + i\vec{k}_\rho\vec{\rho} - i\omega t\right)dk_\rho d\phi_k d\omega, \quad (3)$$

$$\begin{Bmatrix} A_z^{(s3)} \\ \Phi^{(s3)} \end{Bmatrix} = \frac{q}{2\pi^2 V}\int_0^{+\infty}\int_0^{2\pi}\int_{-\infty}^{+\infty} V_3\begin{Bmatrix} -\mu_1/k_z^{(1)} \\ c/\omega\varepsilon_1 \end{Bmatrix} g_1^{-1}k_\rho \times \exp\left(ik_z^{(1)}z + i\vec{k}_\rho\vec{\rho} - i\omega t\right)dk_\rho d\phi_k d\omega, \quad (4)$$

$$\begin{Bmatrix} A_z^{(s21)} \\ \Phi^{(s21)} \end{Bmatrix} = \frac{q}{2\pi^2 V}\int_0^{+\infty}\int_0^{2\pi}\int_{-\infty}^{+\infty} V_{21}\begin{Bmatrix} \mu_2/k_z^{(2)} \\ c/\omega\varepsilon_2 \end{Bmatrix} g_2^{-1}k_\rho \times \exp\left(ik_z^{(2)}z + i\vec{k}_\rho\vec{\rho} - i\omega t\right)dk_\rho d\phi_k d\omega, \quad (5)$$

$$\begin{Bmatrix} A_z^{(s23)} \\ \Phi^{(s23)} \end{Bmatrix} = \frac{q}{2\pi^2 V}\int_0^{+\infty}\int_0^{2\pi}\int_{-\infty}^{+\infty} V_{23}\begin{Bmatrix} -\mu_2/k_z^{(2)} \\ c/\omega\varepsilon_2 \end{Bmatrix} g_2^{-1}k_\rho \times \exp\left(-ik_z^{(2)}z + i\vec{k}_\rho\vec{\rho} - i\omega t\right)dk_\rho d\phi_k d\omega, \quad (6)$$

where

$$k_z^{(i)} = \sqrt{\omega^2 c^{-2}\varepsilon_i\mu_i - k_\rho^2}, \quad \operatorname{Im} k_z^{(i)} \geqslant 0,$$
$$g_i = k_\rho^2 + \frac{\omega^2}{V^2} - \frac{\omega^2}{c^2}\varepsilon_i\mu_i, \quad i = 1, 2. \quad (7)$$

The index $(s1)$ indicates the region $z < 0$, the index $(s2)$ indicates the layer region $0 < z < d$, and the index $(s3)$ indicates the region $z > d$. The boundary conditions give the following expressions for the coefficients:

$$V_1 = \frac{\omega(\varepsilon_1 g_1 - \varepsilon_2 g_2)}{c\varepsilon_2 g_2} + \frac{\varepsilon_1 k_z^{(2)}\tau_+}{\varepsilon_2 g_2 \varkappa_+} + \frac{2\varepsilon_1 k_z^{(1)}k_z^{(2)}}{g_2\varkappa_+}\left[\frac{\varkappa_+}{\varkappa_-}\exp\left(-2ik_z^{(2)}d\right) - \frac{\varkappa_-}{\varkappa_+}\right]^{-1} \times \left[\frac{\tau_-}{\varkappa_-}\exp\left(i\omega d - ik_z^{(2)}d\right) - \frac{\tau_+}{\varkappa_+}\right], \quad (8)$$

$$V_{21} = \frac{k_z^{(2)}\tau_+}{g_1\varkappa_+} - \frac{\varkappa_- k_z^{(2)}}{\varkappa_+ g_1}\left[\frac{\varkappa_+}{\varkappa_-}\exp\left(-2ik_z^{(2)}d\right) - \frac{\varkappa_-}{\varkappa_+}\right]^{-1}, \quad (9)$$

$$V_{23} = \frac{k_z^{(2)}}{g_1}\left[\frac{\varkappa_+}{\varkappa_-}\exp\left(-2ik_z^{(2)}d\right) - \frac{\varkappa_-}{\varkappa_+}\right]^{-1} \times \left[\frac{\tau_-}{\varkappa_-}\exp\left(i\omega d - ik_z^{(2)}d\right) - \frac{\tau_+}{\varkappa_+}\right], \quad (10)$$

$$V_3 = \frac{\exp(i\omega d - ik_z^{(1)}d)}{\varepsilon_2 g_2}\left[\frac{\omega}{c}(\varepsilon_1 g_1 - \varepsilon_2 g_2) + \frac{\varepsilon_1 k_z^{(2)}\tau_-}{\varkappa_-}\right] - \frac{2\varepsilon_1 k_z^{(1)}k_z^{(2)}}{g_2}\left[\frac{\varkappa_+}{\varkappa_-}\exp\left(-2ik_z^{(2)}d\right) - \frac{\varkappa_-}{\varkappa_+}\right]^{-1} \times \frac{\tau_-}{\varkappa_-^2}\exp\left(i\frac{\omega}{V}d - ik_z^{(1)}d - 2ik_z^{(2)}d\right), \quad (11)$$

where

$$\varkappa_\pm = \varepsilon_1 k_z^{(2)} \pm \varepsilon_2 k_z^{(1)},$$
$$\tau_\pm = \frac{\omega}{c}(\varepsilon_2 g_2 - \varepsilon_1 g_1) \pm \beta k_z^{(1)}\varepsilon_2(g_2 - g_1). \quad (12)$$

Note that the integral over ϕ_k can be calculated using the formula $\int_0^{2\pi} e^{i\vec{k}\vec{\rho}}d\phi_k = 2\pi J_0(k_\rho\rho)$.

The field components are determined by the formulas

$$\vec{E} = -\nabla\Phi - \frac{1}{c}\frac{\partial\vec{A}}{\partial t}, \quad \vec{B} = rot\,\vec{A}. \quad (13)$$

We consider the magnetic field strength in region 3:

$$\vec{H} = H_\phi\vec{e}_\phi = \left(H_\phi^{(3)} + H_\phi^{(s3)}\right)\vec{e}_\phi,$$
$$H_\phi^{(3)} = \frac{iq}{2c}\int_{-\infty}^{+\infty} d\omega s_1 H_1^{(1)}(s_1\rho)\exp\left(i\frac{\omega z}{V} - i\omega t\right),$$
$$H_\phi^{(s3)} = \frac{q}{\pi V}\int_{-\infty}^{+\infty} dk_\rho\int_{-\infty}^{+\infty} d\omega\frac{\exp\left(ik_z^{(1)}z - i\omega t\right)}{g_1 k_z^{(1)}} \times k_\rho^2 H_1^{(1)}(k_\rho\rho)V_3, \quad (14)$$

where $s_1(\omega) = \sqrt{\omega^2(\varepsilon_1\mu_1\beta^2 - 1)/V^2}$ $[\operatorname{Im} s_1(\omega) \geqslant 0]$, and $H_1^{(1)}(k_\rho\rho)$ is the Hankel function. Note that we can integrate (14) on the half-axis only using the formula $\int_{-\infty}^{+\infty} f(\omega)d\omega = 2\int_0^{+\infty}\operatorname{Re}[f(\omega)]d\omega$, which follows from the reality of the field components.

III. APPROXIMATE SOLUTION FOR A DIELECTRIC PLATE

In accordance with the approximate method under consideration, the field in the object without "external" boundaries should be found first. In the case of the plane layer, it is the field of the charge in an infinite medium 2. This field is determined by a formula analogous to (14):

$$H_{\phi}^{(2)} = \int_{-\infty}^{+\infty} d\omega H_{\phi\omega}^{(2)} \exp(-i\omega t),$$
$$H_{\phi\omega}^{(2)} = \frac{iq}{2c} s_2(\omega) H_1^{(1)}[s_2(\omega)\rho] \exp\left(i\frac{\omega z}{V}\right), \tag{15}$$

where $s_2(\omega) = \sqrt{\omega^2(\varepsilon_2\mu_2\beta^2 - 1)/V^2}$ [$\mathrm{Im}\, s_2(\omega) \geqslant 0$].

The method under consideration allows the small wavelength waves to be analyzed ($d\sqrt{\varepsilon_2\mu_2}\omega/c \gg 1$). At the boundary, $z = d$, we have approximately for these frequencies

$$H_{\phi\omega}^{(2)}|_{z=d} \approx \frac{iq}{c}\sqrt{\frac{s_2}{2\pi\rho}} \exp\left(i\frac{\omega d}{V} + is_2\rho_* - i\frac{3\pi}{4}\right), \tag{16}$$

where $\rho_* = \rho - (z-d)\tan\theta_t$, and θ_t is a transmission angle determined by Snell's law:

$$\sin\theta_t = \frac{\sin\theta_i\sqrt{\varepsilon_2\mu_2}}{\sqrt{\varepsilon_1\mu_1}}. \tag{17}$$

In the case under consideration, the angle of incidence θ_i is equal to the Cherenkov angle θ_p (Fig. 1):

$$\theta_i = \theta_p = \arccos[(\sqrt{\varepsilon_2\mu_2}\beta)^{-1}]. \tag{18}$$

The amplitude of the first refracted wave is determined by the Fresnel transmission coefficient [6]

$$T = \frac{2\sqrt{\frac{\mu_1}{\varepsilon_1}}\cos\theta_t}{\sqrt{\frac{\mu_2}{\varepsilon_2}}\cos\theta_i + \sqrt{\frac{\mu_1}{\varepsilon_1}}\cos\theta_t}. \tag{19}$$

Note that the transmitted wave is cylindrical, as is the incident wave, i.e., the divergence of the ray tube is the same as in the layer, and the amplitude decreases with $1/\sqrt{\rho}$. Taking into account (16), the field in region 3 has the following form:

$$H_{\phi}^{(3)}(\omega) = \frac{iq}{c} T\sqrt{\frac{s_2(\omega)}{2\pi\rho}} \exp\left[i\omega\frac{d}{V} + is_2(\omega)\rho_* + il\frac{\omega}{c}\sqrt{\varepsilon_1\mu_1} - i\frac{3\pi}{4}\right], \tag{20}$$

where $l = (z-d)/\cos\theta_t$ is the path of the wave in region 3.

The results obtained on the basis of the exact and approximate formulas are shown in Fig. 2. We see that the results are close even for $d = 2\lambda_2$ (in the zone of the first ray). In the case where $d \sim 10\lambda_2$, very good agreement is shown for the majority of "the light bar." This fact stimulates the application of this method to more complex objects where the exact solution cannot be found.

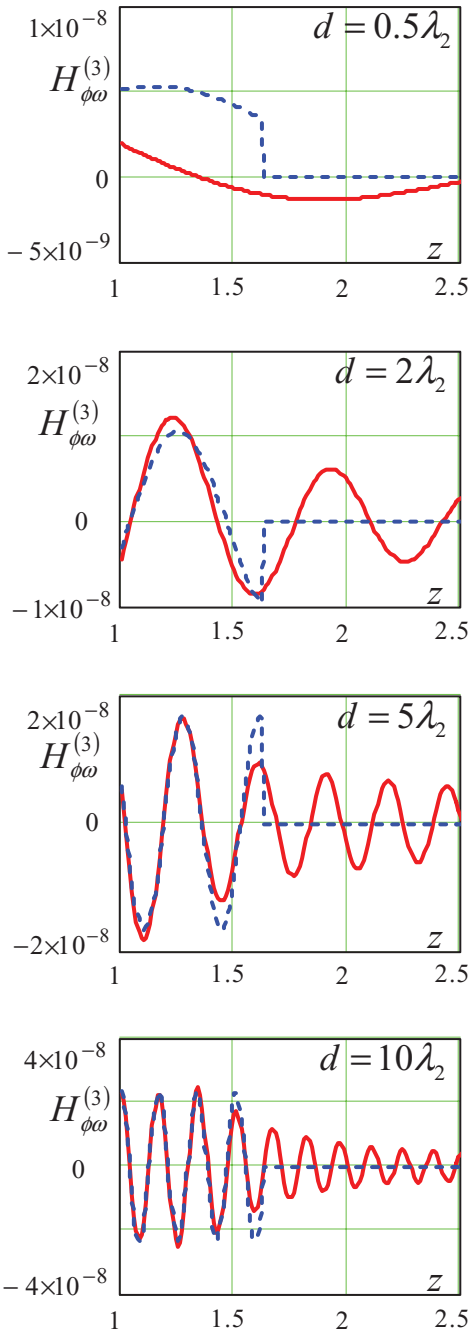

FIG. 2. (Color online) Fourier component of the magnetic field strength $H_{\phi\omega}^{(3)}$ (in A s/m) as a function of z; computations are performed using the exact (solid curves) and approximate (dashed curves) formulas; $\varepsilon_2 = 1.5$, $\mu_2 = 1$, $q = -1$ nC, $\beta = 0.99$, $\rho = 0.6$ cm.

IV. APPROXIMATE METHOD FOR A CONE

In this section, the method under consideration is applied to the case of an infinite cone with a cylindrical vacuum channel (Fig. 3). The permittivity and permeability of the cone material are $\varepsilon_2 = \varepsilon$ and $\mu_2 = \mu$, respectively, and the channel and the region outside the cone are in a vacuum: $\varepsilon_1 = \mu_1 = 1$. The geometry of the problem gives the external boundary of the cone determined by the equation $\rho = (z_0 - z)\tan\alpha$, where $0 < \alpha < \pi/2$. A point charge moves along the axis (z axis) of the channel of radius a, which can either be smaller or larger than the typical wavelengths (the case of relatively small radius $a < \lambda$ is of the most interest). It is also assumed that the CR

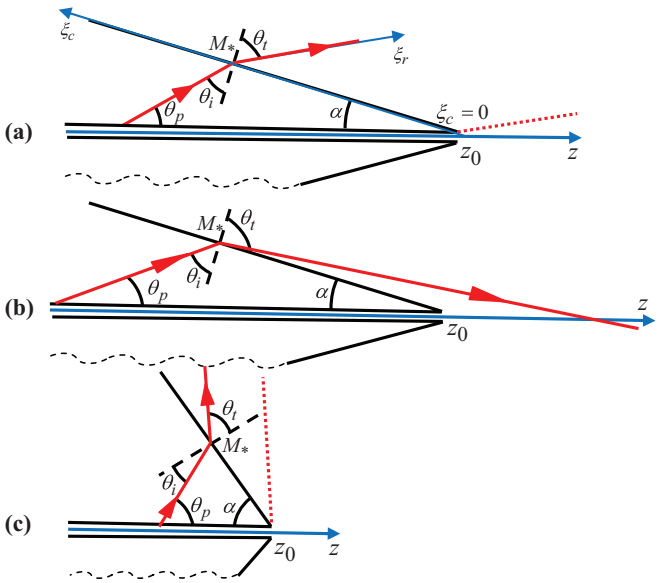

FIG. 3. (Color online) Cross section of the cone for different ray dispositions; $\theta_{i,t} > 0$ in (a) and (b); $\theta_{i,t} < 0$ in (c).

wave travels a distance in the dielectric much longer than the wavelength under consideration.

First, the problem should be solved for the case of an infinite medium with a vacuum channel. The solution of this problem is known [8]: the Fourier transform of the magnetic field can be written in the form

$$H^{(2)}_{\phi\omega} = \frac{iq}{2c}\eta s H_1^{(1)}(s\rho)\exp\left(i\frac{\omega}{V}z_*\right), \tag{21}$$

where

$$\eta = -\frac{2i}{\pi a}\left[\frac{1-\varepsilon\mu\beta^2}{\varepsilon(1-\beta^2)}I_1(ka)H_0^{(1)}(sa) + sI_0(ka)H_1^{(1)}(sa)\right]^{-1},$$
$$s = \omega V^{-1}\sqrt{\varepsilon\mu\beta^2-1}, \quad (\mathrm{Im}\, s \geqslant 0), \tag{22}$$
$$k = |\omega|V^{-1}\sqrt{1-\beta^2}.$$

Additionally, it is necessary to determine the point of incidence M_* for the wave on the cone boundary. The coordinates of the incidence point ρ_*, z_* are a function of the coordinates of the observation point. Analysis of the ray geometry (Fig. 3) gives the following results:

$$\rho_* = (z_0 - z_*)\tan(\alpha), \quad z_* = \frac{z_0\tan(\alpha) + z\cot(\alpha+\theta_t) - \rho}{\tan(\alpha)+\cot(\alpha+\theta_t)},$$
$$\sin\theta_t = \sqrt{\varepsilon\mu}\sin\theta_i, \quad \theta_i = \frac{\pi}{2} - \alpha - \theta_p, \tag{23}$$
$$\cos\theta_p = 1/(\sqrt{\varepsilon\mu}\beta).$$

It is assumed that the volume wave exists outside the cone; that is, total reflection does not occur, i.e., the condition $\sqrt{\varepsilon\mu}\sin|\theta_i| < 1$ is fulfilled.

Note that angles θ_i and θ_t have the same sign, they can be either positive or negative simultaneously. Figures 3(a) and 3(b) illustrate the case $\alpha + \theta_p < \pi/2$ (when $\theta_{i,t} > 0$); the opposite case $\alpha + \theta_p > \pi/2$ (when $\theta_{i,t} < 0$) is characterized by the different positional relationship of the rays and the vector normal to the boundary [Fig. 3(c)].

One can show that the divergence of the ray tube outside the cone is the same as in the cone, which is explained by the cylindrical character of the wave field. As a result, we obtain the expression for the field outside the cone in the form

$$H_{\phi\omega} \approx H^{(2)*}_{\phi\omega}\sqrt{\frac{\rho_*}{\rho}}\, T\exp(i\omega l/c), \tag{24}$$

where $H^{(2)*}_{\phi\omega}(\omega)$ is the incident field (21) at the point M_*, T is the Fresnel transmission coefficient (19), and l is the ray path in vacuum:

$$l = (z - z_*)/\sin(\alpha+\theta_t). \tag{25}$$

Naturally, the obtained result describes the field outside the cone in the zone in which the transmitted wave exists. If $\alpha + \theta_t < \pi/2$, then this zone is bounded:

$$z < z_0 + \rho\tan(\theta_t + \alpha\,\mathrm{sgn}\,\theta_t) \tag{26}$$

[dotted lines in Figs. 3(a) and 3(c)]. However, if $\alpha + \theta_t > \pi/2$, then the transmitted wave exists everywhere outside the cone [Fig. 3(b)]. One can show that this inequality is equivalent to the following:

$$\tan\alpha < (1-\beta)/\sqrt{\varepsilon\mu\beta^2-1}. \tag{27}$$

Under this condition, the transmitted wave propagates to the z axis, so the field increases along the ray [Fig. 3(b)]. Formally, in this case, the ray optical solution tends to infinity if $\rho \to 0$, according to (24). Naturally, our approximate solution is not true at small ρ where the wave amplitude depends strongly on distance. Practically, the solution obtained here is correct for $\rho > 2\pi c/\omega$.

An important characteristic of radiation is the spectral density of energy passing through a unit square. This value can be introduced in the following way. We consider the total energy flowing through a unit square: $\Sigma = \int_{-\infty}^{+\infty} S dt$, where $S = c(4\pi)^{-1}|[\vec{E}, \vec{H}]|$ is the modulus of the Poynting vector. Because in the approximation under consideration the magnetic and electric strengths are mutually orthogonal and $|\vec{E}| = |\vec{H}| = |H_\phi|$, we have

$$\Sigma = c(4\pi)^{-1}\int_{-\infty}^{+\infty}|H_\phi|^2 dt = \frac{c}{4\pi}\iiint_{-\infty}^{+\infty} H_{\phi\omega}H_{\phi\omega'} \times \exp[-i(\omega-\omega')t]d\omega' d\omega dt. \tag{28}$$

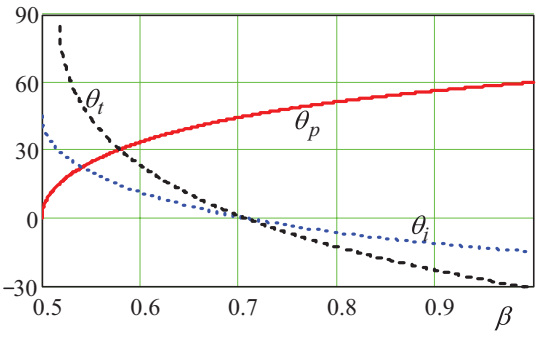

FIG. 4. (Color online) Angle of the CR, angle of incidence, and angle of refraction (in degrees) as functions of the charge velocity for $\alpha = 45°$.

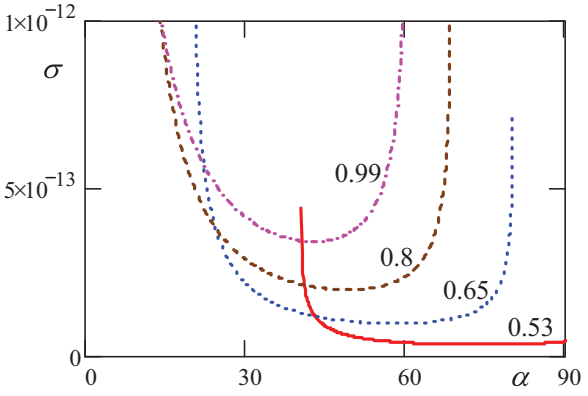

FIG. 5. (Color online) Spectral density of the radiation energy σ (J s/m^2) on the cone surface at a distance $\xi_c = 5$ cm from the cone vertex as a function of α for different β, indicated near the curves.

Applying the formula $\int_{-\infty}^{+\infty} \exp[-i(\omega - \omega')t]\,dt = 2\pi\delta(\omega - \omega')$ and the equality $H_{\phi,-\omega} = \overline{H}_{\phi\omega}$ (where the upper line indicates the complex conjugate), after a simple transformation, we obtain

$$\Sigma = \int_0^{+\infty} \sigma\, d\omega = \int_0^{+\infty} c|H_{\phi\omega}|^2 d\omega, \tag{29}$$

where $\sigma = c|H_{\phi\omega}|^2$ is the spectral density of energy flowing through a unit square. Using (24) we have

$$\sigma \approx \left|T H^{(2)*}_{\phi\omega}\right|^2 \rho_*/\rho. \tag{30}$$

V. RESULTS OF COMPUTATION FOR THE CONE

All computations were performed with the following parameters: $\varepsilon = 4$, $\mu = 1$, $a = 2$ mm, $q = -1$ nC, and $\omega = 2\pi \times 3 \times 10^{10}$ s^{-1}. Note that we present here results for case of nonmagnetic objects because such objects are typical for applications.

Figures 4–8 illustrate some properties of the field obtained above. Figure 4 shows the angle of the CR, the incidence angle, and the angle of refraction as a function of the charge velocity. Recall that the positive values of θ_i and θ_t correspond to the case shown in Figs. 3(a) and 3(b), and negative values of these angles correspond to the case shown in Fig. 3(c).

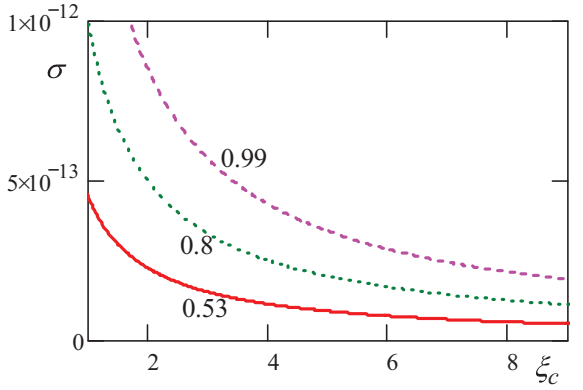

FIG. 6. (Color online) Spectral density σ (J s/m^2) as a function of the distance ξ_c (cm) from the cone vertex along the cone surface; $\alpha = 45^\circ$; values of β are given near the curves.

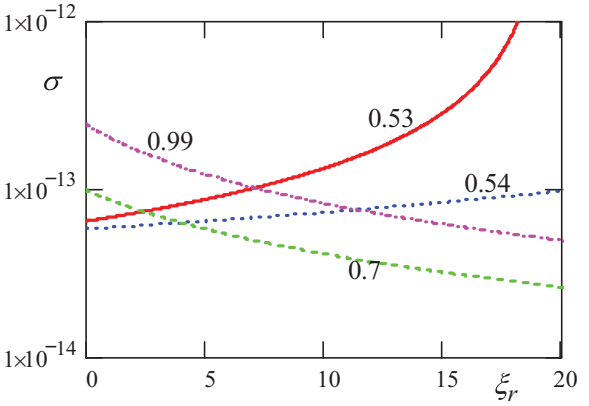

FIG. 7. (Color online) Spectral density σ (J s/m^2) as a function of the distance ξ_r (cm) along the ray from the cone surface: the initial point M_* is situated at $\rho_* = 5$ cm; $\alpha = 45^\circ$; values of β are given near the curves.

The dependence of σ on the cone surface for different charge velocities is shown in Fig. 5. Note that there are limiting values of α for each curve, which are explained by the effect of total reflection of the CR at the cone boundary. The radiation energy approaches infinity when α approaches one of these limits.

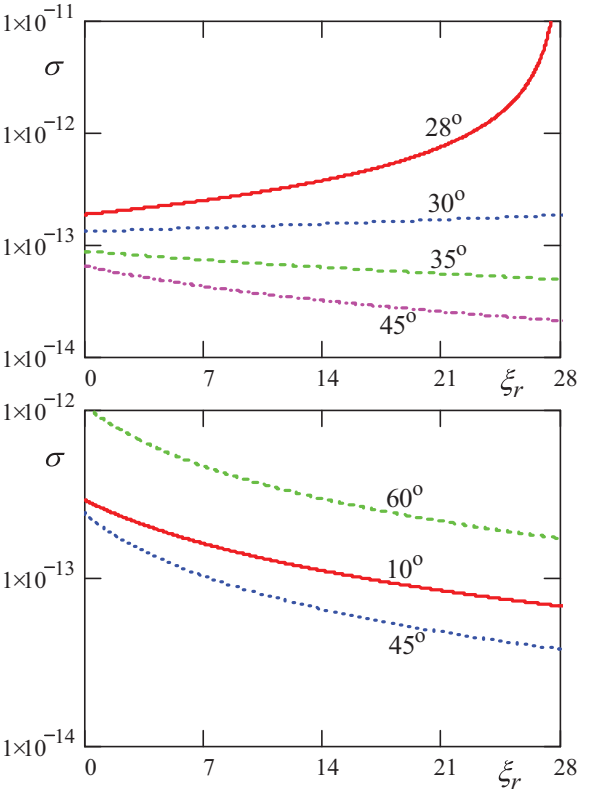

FIG. 8. (Color online) Spectral density σ (J s/m^2) as a function of the distance ξ_r (cm) along the ray from the cone surface: the initial point M_* is situated at $\rho_* = 5$ cm; $\beta = 0.6$ (top); $\beta = 0.99$ (bottom); values of α are given near the curves.

Figure 6 illustrates the typical dependence of the spectral density of the radiation energy on the cone surface on the distance ξ_c from the cone vertex. This dependence monotonically decreases because the CR is a cylindrical divergence wave in the cone.

The typical dependencies of the spectral density of the radiation energy σ on the distance from the cone boundary along the rays are shown in Figs. 7 and 8. One can see that there are some values of the parameters at which the radiation energy increases with distance ξ_r. This means that the radiation is a convergent cylindrical wave [Fig. 3(b)]. As a rule, this effect takes place for velocities close to the Cherenkov threshold, $\beta_C = 1/\sqrt{\varepsilon\mu}$, while for ultrarelativistic velocities the radiation energy decreases along the ray, i.e., the wave is divergent.

VI. CONCLUSION

An approximate method for calculating the radiation from a moving charge in the presence of a dielectric (or magnetic) object has been developed. In the first step of this technique, the field of the charge in an infinite medium without "external" borders is calculated. At this stage, we take into account the wave interaction of the charge field with the "near" boundaries of the object. It is important that the distance from the object boundary to the charge trajectory can be arbitrary, so we can analyze the most interesting case when this distance is relatively small ($<\lambda$). The second step is the approximate calculation of the radiation exiting the object. This calculation is performed with the help of the Fresnel transmission coefficient and the laws of ray optics. As result, we can obtain relatively simple expressions for the wave field components outside the object. Thus, the technique under consideration allows taking into account both the "near" borders of the object and the "distant" ones without cumbersome computations.

As a test problem, the case of a charge crossing a dielectric plate has been considered. Computations of the field have been performed using exact and approximate methods, and the results agree well. Using this method for the case of a conical dielectric object allows the description of some interesting physical phenomena, for example, convergent Cherenkov-transition radiation.

Note that the technique developed here allows us to easily take into account losses in the medium because we can use complex values of ε and μ in the obtained formulas. Moreover, although we considered here the case of point charge, the method under consideration can be applied to particle bunches having different sizes and forms. We believe also that the method will be useful for problems with objects having more complex shapes. As well, in principle, accelerated or nonlinear motion of charge can be considered, but such problems go beyond the scope of this work.

ACKNOWLEDGMENTS

This research was supported by the grant of President of Russian Federation, the Russian Foundation for Basic Research (Grant No. 12-02-31258), and the Dmitry Zimin "Dynasty" Foundation.

[1] V. P. Zrelov, *Vavilov-Cherenkov Radiation in High-Energy Physics* (Israel Program for Scientific Translations, Jerusalem, 1970).

[2] A. P. Potylitsyn, Yu. A. Popov, L. G. Sukhikh, G. A. Naumenko, and M. V. Shevelev, J. Phys.: Conf. Ser. **236**, 012025 (2010).

[3] S. N. Galyamin and A. V. Tyukhtin, Phys. Rev. B **81**, 235134 (2010).

[4] T. Yu. Alekhina and A. V. Tyukhtin, Phys. Rev. ST-AB **15**, 091302 (2012).

[5] V. A. Fok, *Electromagnetic Diffraction and Propagation Problems* (Pergamon, New York, 1965).

[6] S. Solimeno, B. Crosignani, and P. DiPorto, *Guiding, Diffraction, and Confinement of Optical Radiation* (Academic, New York, 1986).

[7] V. L. Ginzburg, *The Propagation of Electromagnetic Waves in Plasma* (Pergamon, London, 1964).

[8] B. M. Bolotovskii, Sov. Phys. Usp. **4**, 781 (1962).